Electronic Spectra and Structures of Solvated NH_4 Radicals, $NH_4(NH_3)_n$ ($n = 1-8$)

Shinji Nonose,[†] Tomokazu Taguchi,[†] Feiwu Chen,[‡,§] Suehiro Iwata,[§,||] and Kiyokazu Fuke*[,†]

Department of Chemistry, Faculty of Science, Kobe University, Kobe 657-8501, Japan, Japan Science and Technology Corporation, Japan, Institute of Molecular Science, Okazaki 444-8585, Japan, and Evaluation of University Education and Research, NIAD, Chiyoda, Tokyo 101-8436, Japan

Received: December 18, 2001; In Final Form: March 20, 2002

Electronic spectra of ammoniated ammonium radicals, $NH_4(NH_3)_n$, produced through the photolysis of ammonia clusters, are investigated with a laser photodepletion spectroscopy. Vibrationaly resolved bands beginning at energy of 9305 ± 15 cm^{-1} are successfully assigned to NH_4NH_3. These bands are ascribed to the $2\ ^2A - 1\ ^2A$ transition derived from the $3p\ ^2F_2 - 3s\ ^2A_1$ excitation of NH_4. A second group of bands beginning at energy 10073 ± 15 cm^{-1} is assigned to the $1^2E - 1^2A$ transition. Electronic spectra of a series of $NH_4(NH_3)_n$ ($n = 1-8$) are also recorded with low resolution in the energy region of 4500−16000 cm^{-1}. A drastic decrease of the excitation energy from 15062 cm^{-1} for NH_4 to 5800 cm^{-1} for $NH_4(NH_3)_4$ is observed, while no appreciable spectral change is found for $n \geq 5$. The large spectral change is ascribed to the spontaneous ionization of NH_4 in ammonia clusters. Successive binding energies of $NH_4(NH_3)_n$ in the excited state are determined from the spectral band positions.

I. Introduction

An ammonium radical NH_4 has been known to be a typical hypervalent Rydberg radical and it is isoelectronic with an alkali atom.[1−7] Because a free NH_4 is unstable and has a very short lifetime,[8] most of spectroscopic studies have been carried out for its isotomer ND_4.[2−5] Porter and co-workers have studied the stability of small $NH_4(NH_3)_n$ by a neutralized ion beam spectroscopy.[9,10] The lifetime of NH_4 in ammonia clusters has also been examined by two-step photoionization experiments with nano- and femtosecond lasers.[8,11] The structure and binding energy of ammoniated NH_4 clusters have also been investigated theoretically by Kassab et al.[12,13]

The existence of NH_4 radical has been speculated in solution, especially in the reaction of solvated electron and in electrochemistry.[14−16] The radical has a loosely bounded valence electron as in the case of alkali atoms. If the radical exists in condensed phase, the Rydberg electron would be substantially influenced by solvent molecules and might be extensively diffused. In relation to this issue, the electronic structure of the polar solvent clusters containing metal atoms has been investigated[17−39] to model microscopic solvation of electrons and metal ions.[17−21] Ionization energies of these clusters have been determined as a function of solvent molecules.[22−26] To characterize the electronic structure of an alkali atom in clusters, the photoelectron spectra of negatively charged alkali atom−solvent clusters have been examined.[25−31] Recently, Schulz's and our group have also measured the electronic absorption spectra of solvent clusters containing alkali atoms such as Na[32,33] and Li.[34] The geometric and electronic structures of these clusters have also been studied using various theoretical methods.[35−39] Both experimental and theoretical results indicate the spontaneous ionization of the metal atom in small clusters; the alkali metal atom is ionized to form the one-center ionic state with increasing the cluster size. Since NH_4 is isoelectronic with an alkali atom, ammoniated NH_4 clusters may serve a new system to investigate the electron localization mode in clusters. In our previous works, the ionization energies of $NH_4(NH_3)_n$ have been determined by photoionization threshold measurements.[40,41] We have also reported the preliminary results on the photodepletion spectra of $NH_4(NH_3)_n$ ($n = 1-4$).[42]

In the present work, the electronic absorption spectra of ammoniated NH_4 radicals are investigated by the photodissociation technique in order to get further insight into the electronic structure of an NH_4 in clusters. Vibronic transitions of NH_4-NH_3 derived from the 3p−3s excitation of free NH_4 are examined in the energy region of 9000−11000 cm^{-1}. Calculations on the potential energy surfaces and vibrational frequencies of NH_4NH_3 in the ground and low-lying excited states are also carried out by ab initio methods to assign the observed vibronic bands. The electronic transition of $NH_4(NH_3)_n$ ($n = 1-8$) is also experimentally investigated in the energy region of 4500−16000 cm^{-1}. On the bases of these results, the mechanism of stabilization of NH_4 and the localization mode of the Rydberg electron in ammonia clusters are discussed.

II. Experimental Section

The apparatus consists of a cluster source and a reflectron type time-of-flight (TOF) mass spectrometer. Ammonia clusters are generated by supersonic expansion of pure ammonia from a pulsed nozzle (General valve, series 9). Ammonia (NH_3, minimum purity of 99.99%, Nippon Sanso) is used without further purification. $NH_4(NH_3)_n$ are produced through the photodissociation of ammonia clusters at 193 nm by using an ArF excimer laser (Lamda Physik, COMPeX100) as the photolysis laser.[40−42] Photodepletion spectra are recorded in the energy region of 4500−16000 cm^{-1} by measuring depletion of each cluster ion with a pump laser. We use two light sources as the pump laser: one is an idler output of an optical parametric oscillator (Spectra Physics, MOPO-730) and the other is an

* To whom correspondence should be addressed.
† Department of Chemistry.
‡ Japan Science and Technology Corporation.
§ Institute of Molecular Science.
|| Evaluation of University Education and Research.

10.1021/jp0145457 CCC: $22.00
Published on Web 05/03/2002

TABLE 1: The Geometric Parameters, the Binding Energy ΔE, and the Barrier Height of H_3NHNH_3

state	method/basis set	N_I-H_{center}[a]	N_I-N_{II}[a]	ΔE[b]	ΔH_{298}[b]	barrier[b]
cation	MP2/AVTZ	1.117	2.697	−25.2	−25.8	0.72 (3.5)[c]
cation[d]	MP2/6-311++(d,p)	1.120	2.694	−27.6	−27.1	
cation	Exper.		2.69 (5)[e]		−24.8[f]	
cation TS	MP2/AVTZ	1.300	2.600			
neutral 1^2A	MP2/AVTZ	1.059	2.866	−5.3	−5.9	1.79 (8.5)[c]
neutral 1^2A TS	MP2/AVTZ	1.292	2.584			
neutral 2^2A	SCI/AVTZ	1.084	2.711	−24.5		(5.4)[c]
neutral 1^2E	SCI/AVTZ	1.038	2.873	−24.0		(18.2)[c]

[a] Unit: angstrom. [b] Unit: kcal/mol. [c] Only two distances N_I-N_{II} and N_I-H_{center} are optimized and the other geometric parameters are fixed at the staggered $H_3N_I-H_{center}-N_{II}H_3$, and they are upper-bound to the real barrier height. [d] Reference 45. [e] Reference 46. [f] Reference 47.

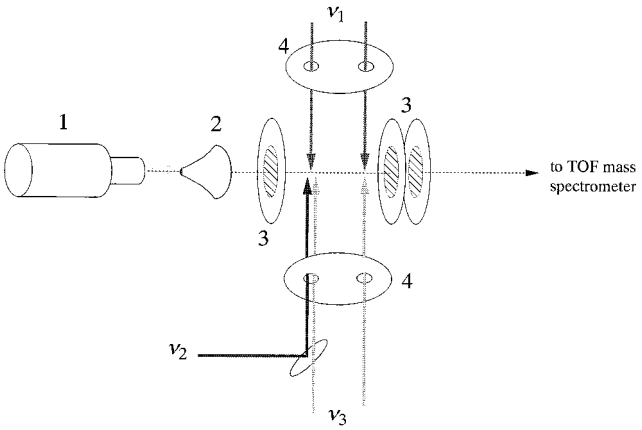

Figure 1. Schematic drawing of the setup for dual beam configuration; (1) pulsed nozzle, (2) skimmer, (3) acceleration plates, (4) pinhole. The photolysis (ν_1) and probe (ν_3) lasers are split into dual beams, and introduced collinearly and counterpropergatedly to an acceleration region of the time-of-flight mass spectrometer, while the pump laser beam (ν_2) is introduced collinearly with one of the beams.

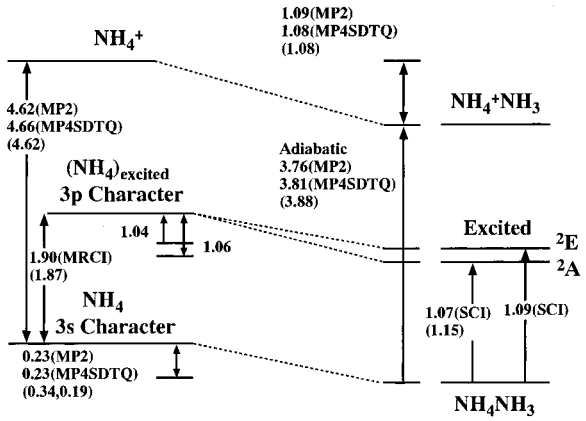

Figure 2. The adiabatic energy diagram of NH_4 and NH_4NH_3 (in eV). In parentheses, the experimental values[40] are given. The excitation energy of NH_4 has been calculated with a multireference CI level in ref 50.

output of the difference frequency generation of a dye laser (Quanta Ray, PDL-3) and a YAG fundamental (1064 nm). After the irradiation of the pump laser, the clusters remained in the molecular beams are probed by photoionization with the third (355 nm) or fourth harmonic (266 nm) of a YAG laser (Spectra Physics, GCR-250). Delay time between the photolysis and pump lasers is 0.1−16 μs, while that between the pump and probe lasers is typically 10−50 ns. To improve an S/N ratio, we adopt a dual beam configuration as shown in Figure 1. Both the photolysis and probe laser beams are split into dual beams, and are introduced collinearly and counterpropergatedly to an acceleration region of the mass spectrometer, while the pump laser beam is introduced collinearly with one of the beams. The cluster ions produced are accelerated and are introduced to a field-free region of the TOF mass spectrometer. The ions are reflected by electric fields at the end of the TOF chamber and are detected by a dual micro channel plate after flying back into the field-free region. For the measurement of vibronic spectrum of NH_4NH_3 complex, the ion signal is integrated by a boxcar averager (Stanford Research, SR250). The gate of the boxcar averager is fixed at the flight time of NH_4NH_3, while scanning the wavelength of the pump laser continuously in the energy region of 9000−11000 cm^{-1}. For the measurements of a low-resolution spectrum, the output signals are fed into a digital storage oscilloscope (Iwatsu 9242A) after being amplified by a wide-band amplifier (NF Electronic Instruments, BX-31).

Relative photoabsorption cross section, σ_{rel}, is determined by

$$\sigma_{rel} = \ln (I_{off}/I_{on}) \quad (1)$$

where I_{on} and I_{off} are the signal intensities of ions in the mass spectrum with and without irradiating the pump laser beam, respectively.

III. Theoretical

In all of calculations, the basis set used is aug-cc-pVTZ.[43] GAUSSIAN 98 program package,[44] registered at Computer Center of Institute for Molecular Science, is used. To study the excited states, the single excitation configuration interaction (SCI) level of approximation is used. Some of the optimized geometric parameters are summarized in Table 1 together with the barrier height of the hydrogen transfer. In Figure 2, the relative adiabatic energies are summarized for NH_4NH_3 and its cation.

IV. Results and Discussion

IV.1. Spectrum of NH_4NH_3 Complex. NH_4NH_3 is a prototype of hydrogen bonded complexes and is an interesting target to explore the electronic structure and stability of NH_4. Although a free NH_4 has known to be short-lived (14 ps),[8] the radical is substantially stabilized upon complex formation and its lifetime is elongated more than 10^5 times (2 μs). Since NH_4NH_3 is produced by the photolysis of larger ammonia clusters, it is difficult to cool the complex under an isolated condition in supersonic molecular beam. However, the complex is metastable and dissociates into H atom and ammonia molecules through tunneling if the complex is internally excited. Thus we would expect to observe cooled complexes if we detect them at much longer time after the photolysis. Figure 3 shows the time-dependent spectrum of NH_4NH_3 in the energy region of 9800−10100 cm^{-1} recorded at various delay times between the photolysis and the pump lasers. With increasing the delay time

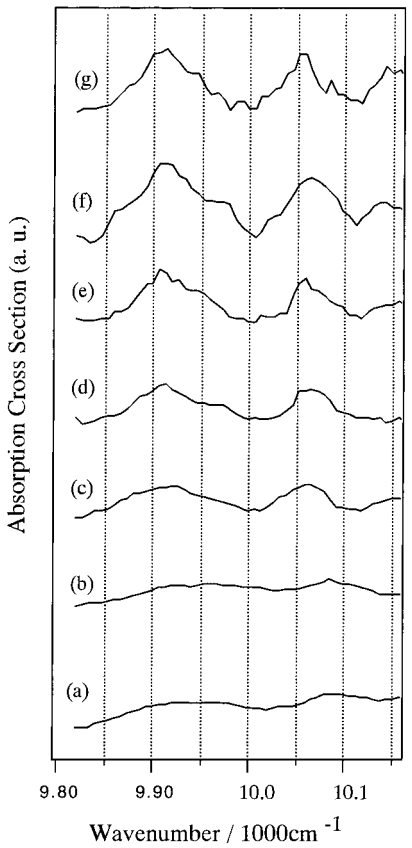

Figure 3. Absorption spectra of NH_4NH_3 complex in the energy region of 9800−10100 cm^{-1} recorded at various delay times. Delay times between the photolysis and pump lasers are 0.1 μs (a), 0.2 μs (b), 0.5 μs (c), 2 μs (d), 7 μs (e), 10 μs (f), and 16 μs (g), respectively.

from 0.1 to 16 μs, the bandwidth decreases gradually without changing the band positions. At the delay time of 16 μs, the bandwidth becomes as small as about 30 cm^{-1}. The apparent time-dependent spectral narrowing clearly indicates that the complexes with lower internal temperature (energy) survive for a longer time and are detected.

Figure 4 shows the vibrationally resolved spectrum of NH_4-NH_3 in the energy region of 9000−11000 cm^{-1} recorded with the delay time of 16 μs. The spectrum is normalized to the intensity of the pump laser beam, which is carefully attenuated to avoid multiphoton absorption. The 3p−3s transition of NH_4 in the visible region has been studied extensively and its band origin is located at 15062 cm^{-1}.[1] Upon complex formation, the spectrum derived from this transition is expected to shift to the red as in the case of the isoelectronic system such as Li(NH_3) and Na(NH_3).[17,25,26] For Li(NH_3), the vertical photodetachment transitions to the neutral ground and first excited states derived from the ^{2}S and ^{2}P level of Li atom are observed at 0.56 and 2.05 eV, respectively, in the photoelectron spectrum of Li^-(NH_3).[25] Since the ^{2}S−^{2}P energy separation of Li atom is 14904 cm^{-1}, the amount of red shift is determined to be 2900 cm^{-1}. From the comparison with these results of Li^- (NH_3), the observed bands of NH_4NH_3 are assigned to those derived from the 3p−3s transition of NH_4. The spectrum exhibits a strong band at 9305 ± 15 cm^{-1} and various vibronic bands in the higher energy region of this band. We also examine the spectrum in the energy region below 500 cm^{-1} from this band, however, no additional absorption peak is observed. Thus, we assign the peak at 9305 ± 15 cm^{-1} to the origin band of the lowest excited state. This band is shifted to the red by more than 5700 cm^{-1} (0.71 eV) with respect to that of NH_4.

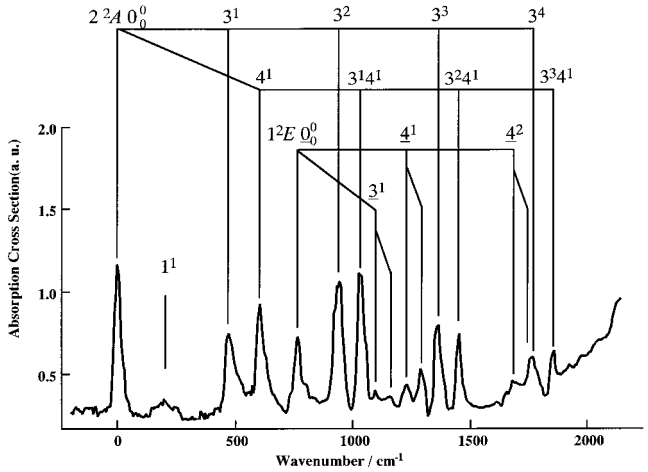

Figure 4. Absorption spectrum of NH_4NH_3 in the energy region of 9000−11000 cm^{-1}. Two electronic transitions are observed, which are assigned to the 2^2A-1^2A and 1^2E-1^2A excitations by comparison with the theoretical calculations. The origin of the 2^2A-1^2A transition is located at 9305 ± 15 cm^{-1}. The main progressions are assigned to the intermolecular bending modes. The 768 cm^{-1}-band is assigned to the origin of the 1^2E-1^2A transition. Vibrational bands in the 1^2E state are indicated with underlines.

To assign the observed spectrum, we calculate the geometries and electronic structures of the complex in the ground and low-lying excited states. The ground state of NH_4 is a 3s $^2A_1$ state, and the excitation of the p orbitals results in the 3p $^2F_2$ excited states; the excitation energy of the 0−0 band of NH_4 is 15062 cm^{-1} (1.87 eV).[1] The calculations predict that NH_4NH_3 has C_3 symmetry with an N−H−N hydrogen bond both in the ground and first excited electronic states. Interaction of NH_4 with an ammonia molecule causes the splitting of three p orbitals. In C_3 symmetry, the ground state of NH_4NH_3 is the totally symmetric 1^2A state, arising from the interaction of the 3s Rydberg orbital with the lone pair orbital on NH_3, while the excited states are the ^2A (z) and ^2E (x, y) symmetries with the z axis as the symmetry axis. The observed bands may correspond to the transitions from the ground state to these excited states. The calculated vertical excitation energies at the geometry of the MP2 level predict the excitation energy of the 2^2A state as about 9000 cm^{-1}, and that of the 1^2E state as about 9600 cm^{-1}. The ordering of the 2^2A_1 and 1^2E_1 states is rather unusual, comparing with the isoelectronic systems such as those of many other metal−ligand complexes. For example, in the Mg^+-H_2O and Ca^+-H_2O complexes, the σ-type (2^2A_1) state has found to be the highest energy level among three ^2P manifolds, while the π-type (1^2B_2) state is the lowest.[48,49] This trend is due to the larger repulsive interaction in the 2^2A_1 state, in which the p orbital is on-axis oriented, than in the ground state. On the other hand, the repulsive interaction becomes weakest in the 1^2B_2 state, because the p orbital is perpendicular to the lone-pair orbitals of oxygen atom as mentioned previously. The change in the ordering of these states for NH_4NH_3 cannot be explained by the difference in the electrostatic interaction between the metal p-orbital and nitrogen lone-pair orbital. In relation to this issue, recently, we have found that the 2^2A_1 state of $Li-D_2O$ is stabilized by a partial charge transfer from Li to D_2O through mixing with higher excited states such as an ion-pair state.[34] We expect similar interaction for NH_4NH_3 as in the case of $Li-D_2O$. Therefore, we assign the band at 9305 cm^{-1} (1.15 eV) to the band origin of the 2^2A state. This assignment is also supported by the following discussion on the assignment of vibronic bands.

TABLE 2: Theoretical and Experimental Vibrational Frequencies of NH_4NH_3 in the Neutral Ground and Low-Lying Excited States[a]

	1^2A	2^2A		1^2E		ionic state
	calcd	calcd	exptl	calcd	exptl	calcd
intermolecular stretch, ν_1	220	305	~200	235		314
intermolecular rotation, ν_2	18	25		117		32
intermolecular bend 1, ν_3	219	534	475	259 294	327 390	381
intermolecular bend 2, ν_4	452	701	607	483 510	460 520	586

[a] The vibrational frequencies in the ionic state are also listed for comparison. All values are in cm^{-1}.

TABLE 3: A List of Band Positions Observed in the 2^2A-1^2A and 1^2E-1^2A Photodepletion Spectrum of NH_4NH_3 and Their Assignments[a]

relative frequency	assignment
0	0° (2^2A origin, 9305 ± 15, vac.)
~200	1^1
475	3^1
607	4^1
768	1^2E origin (10073 ± 15)
942	3^2
1031	3^14^1
1095	$\underline{3}^1$ (1^2E + 327)
1158	$\underline{3}^1$ (1^2E + 390)
1228	$\underline{4}^1$ (1^2E + 460)
1288	$\underline{4}^1$ (1^2E + 520)
1359	$\underline{3}^3$
1448	3^24^1
1685	4^2 (1^2E + 917)
1754	$\underline{4}^2$ (1^2E + 986)
1772	$\underline{3}^4$
1854	3^34^1

[a] All values are in cm^{-1} and are relative to the 2^2A origin band at 9305 ± 15 cm^{-1}. The intermolecular stretching, rotation, and two bending modes are denoted as ν_1, ν_2, ν_3, and ν_4, respectively. The vibrational bands in the 1^2E state are indicated with underlines.

The spectrum in Figure 4 exhibits several vibrational bands in the energy region above the 9305 cm^{-1} band. There are no bands in the spectrum, which have to be assigned to the transitions from the vibrationally hot levels in the ground state, and so the observed vibrational bands should be assigned by considering the symmetry of vibronic levels in the excited state. In C_3 symmetry, NH_4NH_3 has four intermolecular vibrational modes; intermolecular stretch (ν_1) and rotation (ν_2) with *a* irreducible representation, and two intermolecular bending modes (ν_3, ν_4) with *e* symmetry. To assign the observed vibrational bands, the harmonic frequencies of the ground and excited states of NH_4NH_3 are calculated with the MP2 and SCI levels of approximation. The theoretical harmonic frequencies for the intermolecular modes in the ground and excited states are summarized in Table 2, along with the experimental frequencies based on the tentative assignment. Because the intermolecular stretching mode is expected to be strongly coupled with the intramolecular stretching mode of the N−H hydrogen bond,[50−54] the potential energy surfaces are calculated and shown in Figure 5. In these surfaces, the geometric parameters other than the N−N and $N-H_{center}$ distances are fixed at the optimized geometry of the ground state $(H_3NH)-NH_3$. The figures indicate the strong coupling of the two coordinates and a large anharmonicity of the intermolecular stretching mode ν_1, whose frequency under the harmonic approximation is 305 cm^{-1} for the first excited state, 2^2A. The observed broad band at ~200 cm^{-1} above the origin band is assigned to this stretching mode, which may be broadened by combining with the internal rotation mode ν_2. The calculated harmonic frequency apparently overestimates the observed frequency, partly because of the large anharmonicity. The calculated equilibrium N−N distance of the first excited state differs from that of the ground state (see Table 1), and therefore, the progression of the ν_1 mode should be observed. However, only the first member is clearly observed in the spectrum. One of the possible reasons for the missing of the higher members of the progression is that the energy becomes higher than the barrier height of the hydrogen transfer. The barrier height estimated from Figure 5 is 5.4 kcal mol^{-1} (1900 cm^{-1}), which is expected to be substantially larger than the real barrier height in the present model calculation.

Two strong bands are found at 475 and 606 cm^{-1} above the origin, which are considered as the fundamental vibrations. They are assigned to the bending *e* modes (ν_3 and ν_4), calculated at 534 and 701 cm^{-1}. As will be mentioned below, the origin of the second excited state, ^2E, lies just above the bands, and therefore, the vibronic coupling might be large. As indicated in the spectrum of Figure 4, the series of the bands are assigned to the overtones of ν_3 (942, 1369, and 1854 cm^{-1}) and the combinations of ν_3 and ν_4 (1031 cm^{-1}). Because the coupling of the bending motion with the hydrogen transfer mode is weak, the progression can persist above the barrier height.

In the spectrum in Figure 4, we also observe a strong band at 10073 ± 15 cm^{-1}; 768 cm^{-1} above the origin of the 2^2A state. Several vibronic bands start from this band. We assign the band to the origin of the transition to the second excited state, 1^2E, because no such low-frequency modes among the intramolecular vibrations are possible. The theoretical calculations predict the occurrence of the second transition to the 1^2E excited state at about 600 cm^{-1} above the 2^2A state (see Figure 2). Since the 1^2E state is degenerated under C_3 symmetry, the Jahn−Teller distortion is expected. In fact, the N−H−N hydrogen bond in this state is slightly bent in the calculation, but the distortion energy is smaller than the zero-point vibrational levels of the bending modes; it is so-called dynamical Jahn−Teller. As a result, the vibrational levels of ν_3 and ν_4 are split into four vibrational levels; the calculated frequencies are 259, 294, 483, and 510 cm^{-1}. The weak bands at 327 and 390 cm^{-1} above the 10073 cm^{-1} origin are tentatively assigned to the vibronic transitions derived from the ν_3 mode. On the other hand, the bands observed at 460 and 520 cm^{-1} are assigned to the transitions to the vibrational levels of the ν_4 mode. The calculations underestimate the vibrational frequencies, contrary to the usual trends of the overestimation. More accurate theoretical calculations are required to confirm the assignments. As shown in Figure 4, the spectrum in the energy above 1900 cm^{-1} becomes much broader. In this energy region, we would expect to observe several intramolecular vibrational transitions of the 2^2A and the 1^2E states. Thus the broader spectral feature in the higher energy region seems to be ascribed to vibrational congestion. Also the couplings of the inter- and intramolecular vibrational modes with the hydrogen transfer mode may become important in this energy region.

IV.2. Electronic Absorption Spectra of $NH_4(NH_3)_n$ (n = 1−8). Figure 6 shows the electronic absorption spectra of $NH_4(NH_3)_n$ (n = 1−8) in the energy region of 4500−16000 cm^{-1}. These spectra are recorded with much shorter delay time compared with that for the 1:1 complex mentioned in the previous section in order to gain the concentration of solvated NH_4. As a result, the spectral resolution becomes not enough to resolve the vibronic transitions. All spectra are normalized to the intensity of the pump laser beam. As shown in Figure 6a, the absorption spectrum of NH_4NH_3 shows an intense

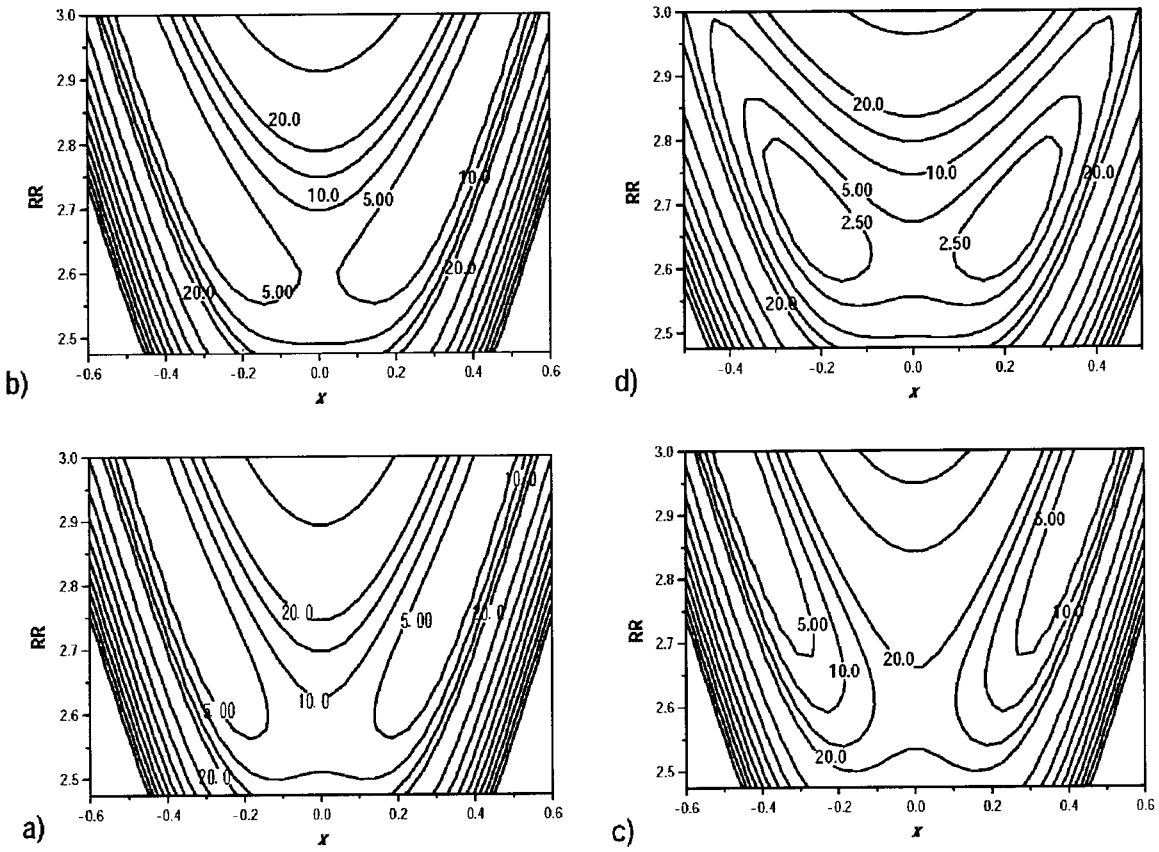

Figure 5. Potential energy surfaces of the ground (a) and two low-lying excited states (b, c) of H_3NHNH_3. For comparison, the surface of the cation (d) is shown. The parameter RR is the N−N distance, and *x* is the displacement of the hydrogen atom from the middle of the N−N bond. The other geometric parameters are fixed at the most stable neutral H_3NHNH_3. The contours are for 5, 10, 15, 20, 40, and 60 kcal/mol from the bottom of the corresponding surface.

maximum at 11700 cm^{-1} and a weak maximum at 15200 cm^{-1}. On the basis of the previous discussion, the former band can be assigned to the transitions to the excited states derived from the ^2P manifolds. The weak band may be assigned to the transition to a higher excited state such as those transitions derived from the 4p Rydberg state of NH_4. The spectrum of $NH_4(NH_3)_2$ exhibits a broad and blue-shaded maximum and its vertical excitation energy is determined as about 9000 cm^{-1}. With the addition of second NH_3, the transition to the 3p-type state is shifted by about 2500 cm^{-1}. The large spectral shift indicates that the second NH_3 also bound directly to NH_4 as predicted by the theoretical calculations.[12] A rather broad bandwidth may be partly due to a large splitting of the 3p-type states. The spectra of $NH_4(NH_3)_3$ and $NH_4(NH_3)_4$ in Parts c and d of Figure 6 show strong peaks at ∼6500 and ∼5800 cm^{-1}, respectively. As seen in these parts of Figure 6, the bandwidth decreases suddenly from $n = 3$ to 4. According to the theoretical calculations, $NH_4(NH_3)_4$ has the structure with T_d symmetry, in which four NH_3 molecules bound to NH_4 through hydrogen bond. In this case, the 3p orbitals of NH_4 interact equivalently with four NH_3 molecules and the splitting of three excited states derived from these orbitals becomes much smaller than those for the smaller clusters. The observed sudden decrease in the bandwidth is consistent with the arguments and shows the filling of the first solvation shell.

Parts e−h of Figures 6 show the spectra of $NH_4(NH_3)_n$ with $n = 5$, 6, 7, and 8, respectively. As seen in these parts of Figure 6, the absorption spectra for $n \geq 5$ show a rather sharp bandwidth and no appreciable change in the band position. In relation to these observations, recently, Schultz and co-workers have reported the absorption spectra of $Na(NH_3)_n$.[33] These spectra show the similar spectral features to those for $NH_4(NH_3)_n$: the rapid decrease in the excitation energy of the lowest transition for $n \leq 4$ and no appreciable change (and/or much smaller increase) in the band position for $n \geq 5$. These results are consistent with those observed in the photoelectron spectra (PES) of negatively charged $Li(NH_3)_n$ and $Na(NH_3)_n$ reported previously by our group.[25,26] In the latter spectra, photodetachment transitions from the anion state to the neutral ground and low-lying excited states derived from the ^2S- and ^2P-type levels of alkali atoms are detected. There are two important characteristics in the PES bands, which can be attributed to the structures having as many Na−N bonds as possible for each *n*. One is that the position of the first band is slightly shifted to lower electron binding energy from $n = 0$ to $n = 1$ and then it becomes relatively constant for larger clusters. These characteristics have been ascribed to the fact that total binding energies of the neutral clusters at their anionic geometries are by 0.12 ($n = 1$)−0.14 ($n = 3$) eV larger than the corresponding values of the anions for each *n*.[30] Another characteristic size dependence of the PES bands, the rapid red-shift of the second band with increasing *n*, has been analyzed in terms of the valence electron distribution. The expected values of the radial distribution (RD) for the unpaired electron of $Na(NH_3)_n$ ($n = 0-4$) at their anionic geometries are calculated having Na at the origin. The R_{max} values, defined as the maximum RD, increase as 4.60, 7.53, 8.77, and 9.68 Bohr for $Na^-(NH_3)_n$ $n = 1-4$, respectively. These numbers indicate that the stepwise enlargement of the valence electron distribution proceeds with ammoniation. The R_{max} of 3^2S-like state for the most stable isomer with the same *n* becomes larger as the number of ammonia molecule increases and exceeds the average Na−H distance in each cluster for *n*

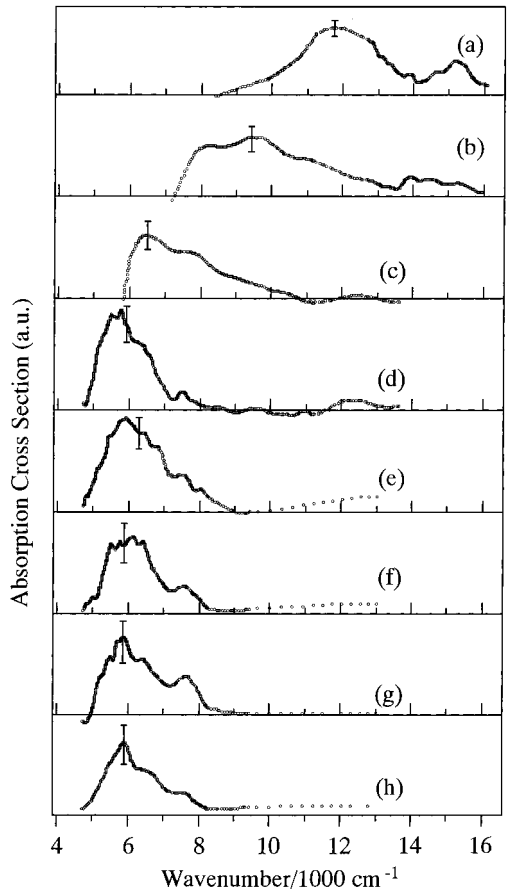

Figure 6. Low-resolution absorption spectra of $NH_4(NH_3)_n$ ($n = 1$ (a)−8 (h)) in the energy region of 4500−16000 cm^{-1}. These spectra are recorded by monitoring the depletion of the cluster ions as a function of the excitation energy. The intensities of the spectra are normalized to the fluence of the pump laser.

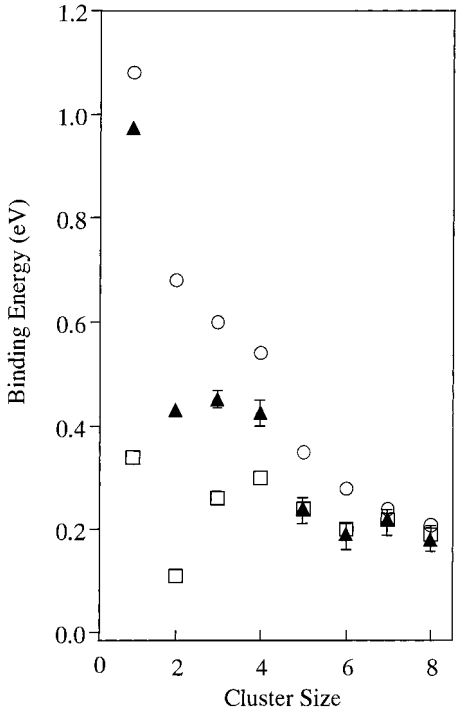

Figure 7. The successive binding energies, $D_{n-1,n}$ [$NH_4(NH_3)_{n-1}-NH_3$], in the excited state, the ground state, and the ionic state are plotted as a function of cluster size n. Filled triangles present the successive binding energies of the ^{2}P-type excited state of $NH_4(NH_3)_n$. The successive binding energies of the neutral ground and those of ionic states are shown by open squares and circles, respectively.

≥ 2. The R_{max}'s of the excited states are also found to increase by a stepwise addition of NH_3 molecules.[30] As a result, the R_{max}'s for 3^2S- and 3^2P-type states in $n = 4$ are about 2.0 and 1.7 times greater than the corresponding atomic values, respectively. The unpaired electron is diffused by the ammoniation not only in the ground state but also in the excited states. In other words, the electronic nature of these neutral clusters with maximum numbers of Na−N bonds changes from the atomic state to the one-center ion-pair state with increasing n: this change is responsible for the rapid decrease of the vertical detachment energy of the transitions to the low-lying excited states. From these results, the rapid decrease in the ^{2}P−^{2}S energy separation of solvated alkali metal atom has been ascribed to the spontaneous ionization of metal atom in clusters.[25,26,33] As mentioned previously, the size dependence of the absorption spectra of $NH_4(NH_3)_n$ is very similar to that for $Na(NH_3)_n$. And also, the size dependence of the ionization energies of $NH_4(NH_3)_n$ is very similar to those for $Li(NH_3)_n$ and $Na(NH_3)_n$. These results strongly suggest that the NH_4 radical is ionized in small ammonia clusters to form the one-center ion pair state, similar to those of $Li(NH_3)_n$ and $Na(NH_3)_n$: the Rydberg electron may be squeezed out over the ammonia molecules when the first shell is closed.[55]

The binding energies of $NH_4(NH_3)_n$ in the neutral ground and ionic states have been determined.[40,56,57] For $NH_4^+(NH_3)_n$, the binding energies are 1.08, 0.68, 0.60, and 0.54 eV for $n = 1-4$, respectively, [56,57] while those in the neutral ground states are 0.34, 0.12, 0.26, and 0.30 eV for $n = 1-4$, respectively.[40] Figure 7 shows the successive binding energies in the 3p-type states, $D_{n-1,n}$ [NH_4*$(NH_3)_{n-1}-NH_3$], together with those of the ground and ionic states.

The binding energy of the 2^2A state is estimated from the band origin at 9305 cm^{-1} in the vibronic spectrum as 0.98 eV, which is close to the calculated value 1.06 eV as is shown in Figure 2. The value is almost equal to that of the cation complex, and is much larger than that of the ground state (0.34 eV). For $2 \leq n \leq 8$, the successive binding energies in the 3p-type states are determined by using the energies at the onsets of each absorption band in the spectra. For $2 \leq n \leq 4$, the binding energies (∼0.44 eV) of the 3p-type state are almost equal to each others. On the other hand, the binding energies decrease suddenly between $n = 4$ and 5. For $n \geq 5$, the binding energies are found to be about 0.2 eV, and are almost the same as those of the ground state.[40] The sudden decrease of the binding energy in the 3p-type state between $n = 4$ and 5 is consistent with the rapid decrease in the ionization energies for $n = 1-4$.[40] These results indicate that the first solvation shell completes with four ammonia molecules as in the case of $NH_4^+(NH_3)_n$ and, for the larger clusters, the extra ammonia molecules are bound to the first shell NH_3 with weaker hydrogen bonds. These arguments are also supported by the theoretical results reported by Evleth and Kassab.[12]

V. Conclusion

The vibrationally resolved electronic spectrum is obtained for the Rydberg radical−molecular complex, NH_4NH_3, with photodepletion experiments. The potential energy surfaces and vibrational frequencies of the ground and the excited states are examined by ab initio calculations. On the bases of these results, the vibronic spectrum of NH_4NH_3 is explained as the excitation of intermolecular bending vibration in the 3p-type states. The electronic excitation energies and intermolecular vibrational

frequencies provide a consistent picture of the structure in this complex. Electronic absorption spectra of $NH_4(NH_3)_n$ ($n = 1-8$) are measured. A drastic decrease of the excitation energy for $n \leq 4$ is observed, while there is no appreciable difference for $n \geq 5$. Successive binding energies of $NH_4(NH_3)_n$ in the 3p-type state decrease monotonically with increasing n. The first solvation shell completes with four NH_3 and further NH_3 is bound to the first shell NH_3 with weaker hydrogen bond. The large spectral change is ascribed to the spontaneous ionization of NH_4 in ammonia clusters.

Acknowledgment. This work is partially supported by the Grant-in-Aid (Grants 11304042) from the Ministry of Education, Science, Sports and Culture of Japan and a JSPS research grant for the Future Program and International Cooperation Program. K.F. is also grateful to the Hyogo Science and Technology Association for partial financial supports. A part of the work is also supported by the project "Computational Chemistry for Molecular Spectroscopies and Chemical Reactions in Atmospheric Environmental Molecules (CCAEM)" of Research and Development Applying Advanced Computational Science and Technology under Japan Science and Technology Corporation (ACT-JST). A part of the calculations were carried out at the Computer Center of the Institute for Molecular Science.

References and Notes

(1) Herzberg, G. *Faraday Discuss. Chem. Soc.* **1981**, *71*, 163.
(2) Herzberg, G. *J. Astrophys. Astron*. **1984**, *5*, 131.
(3) Whittaker, E. A.; Sullivan, B. J.; Bjorklund, G. C.; Wendt, H. R.; Hunziker, H. E. *J. Chem. Phys.* **1984**, *80*, 961.
(4) Watson, J. K. G. *J. Mol. Spectrosc.* **1984**, *107*, 124.
(5) Alberti, F. A.; Huber, K. P.; Watson, J. K. G. *J. Mol. Spectrosc*. **1984**, *107*, 133.
(6) Signorell, R.; Palm, H.; Merkt, F. *J. Chem. Phys.* **1997**, *106*, 6523.
(7) Rodham, D. A.; Blake, G. A. *Chem. Phys. Lett.* **1997**, *264*, 522.
(8) Fuke, K.; Takasu, R. *Bull. Chem. Soc. Jpn.* **1995**, *68*, 3309.
(9) Gellene, G. I.; Cleary, D. A.; Porter, R. F. *J. Chem. Phys.* **1982**, *77*, 3471.
(10) Gellene, G. I.; Porter, R. F. *J. Phys. Chem*. **1984**, *88*, 6680.
(11) Misaizu, F.; Houston, P. L.; Nishi, N.; Shinohara, H.; Kondow, T.; Kinoshita, M. *J. Chem. Phys.* **1993**, *98*, 336.
(12) Kassab, E.; Evleth, E. M. *J. Am. Chem. Soc.* **1987**, *109*, 1653.
(13) Evleth, E. M.; Kassab, E. *Pure Appl. Chem*. **1988**, *60*, 209.
(14) Wan, J. K. S. *J. Chem. Educ*. **1968**, *45*, 40.
(15) Brooks, J. M.; Dewald, R. R. *J. Phys. Chem.* **1971**, *75*, 986.
(16) Kariv-Miller, E.; Nanjundiah, C.; Eaton, J.; Swenson, K. E. *J. Electroanal. Chem.* **1984**, *167*, 141.
(17) Fuke, K.; Hashimoto, K.; Iwata, S. *Adv. Chem. Phys*. **1999**, *110*, 431.
(18) Ohshima, Y.; Kajimoto, O.; Fuke, K. In *Electron Transfer in Chemistry*; Balzani, V., Ed.; Wiley-VCH: New York, 2001; Vol. 4, p 775.
(19) Sanekata, M.; Misaizu, F.; Fuke, K. *J. Chem. Phys*. **1994**, *100*, 1161.
(20) Sanekata, M.; Misaizu, F.; Fuke, K.; Iwata, S.; Hashimoto, K. *J. Am. Chem. Soc*. **1995**, *117*, 747.
(21) Sanekata, M.; Misaizu, F.; Fuke, K. *J. Chem. Phys*. **1996**, *104*, 9768.
(22) Schulz, C. P.; Haugstatter, R.; Tittes, H.-U.; Hertel, I. V. *Z. Phys.* **1988**, *D10*, 279.
(23) Hertel, I. V.; Huglen, C.; Nitsch, C.; Schultz, C. P. *Phys. Rev. Lett*. **1992**, *67*, 1767.
(24) Misaizu, F.; Tsukamoto, K.; Sanekata, M.; Fuke, K. *Chem. Phys. Lett*. **1992**, *188*, 241.
(25) Takasu, R.; Hashimoto, K.; Fuke, K. *Chem. Phys. Lett*. **1996**, *258*, 94.
(26) Takasu, R.; Misaizu, F.; Hashimoto, K.; Fuke, K. *J. Phys. Chem*. **1997**, *A101*, 3078.
(27) Takasu, R.; Taguchi, T.; Hashimoto, K.; Fuke, K. *Chem. Phys. Lett*. **1998**, *290*, 481.
(28) Takasu, R.; Ito, H.; Nishikawa, K.; Hashimoto, K.; Okuda, R.; Fuke, K. *J. El. Sepctros. Relat. Phenom.* **2000**, *106*, 127.
(29) Misaizu, F.; Tsukamoto, K.; Sanekata, M.; Fuke, K. *Surf. Rev. Lett*. **1996**, *3*, 405.
(30) Fuke, K.; Hashimoto, K.; Takasu, R. In *Advances in Metal and Semiconductor Clusters*; Duncan, M. A., Ed.; JAI Press Inc.: Amsterdam, 2000; Vol. 5.
(31) Takasu, R.; Hashimoto, K.; Okuda, R.; Fuke, K. *J. Phys. Chem*. **1999**, *103*, 349.
(32) Schulz, C. P.; Nitsch, C. *J. Chem. Phys*. **1997**, *107*, 9794.
(33) Brockhaus, P.; Hertel, I. V.; Schulz, C. P. *J. Chem. Phys*. **1999**, *110*, 393.
(34) Takasu, R.; Nishikawa, K.; Miura, N.; Sabu, A.; Hashimoto, K.; Schulz, C. P.; Hertel, I. V.; Fuke, K. *J. Phys. Chem*. **2001**, *A105*, 6602.
(35) Hashimoto, K.; Kamimoto, T.; Fuke, K. *Chem. Phys. Lett*. **1997**, *266*, 7.
(36) Hashimoto, K.; Morokuma, K. *J. Am. Chem. Soc*. **1994**, *116*, 11436.
(37) Glendening, E. D. *J. Am. Chem. Soc*. **1996**, *118*, 2473.
(38) Combariza, J. E.; Kestner, N. R.; Jortner, J. *J. Chem. Phys*. **1994**, *100*, 2851.
(39) Barnet, R. N.; Landman, U. *Phys. Rev. Lett*. **1993**, *70*, 1775.
(40) Fuke, K.; Takasu, R.; Misaizu, F. *Chem. Phys. Lett*. **1994**, *229*, 597.
(41) Takasu, R.; Fuke, K.; Misaizu, F. *Surf. Rev. Lett.* **1996**, *3*, 353.
(42) Nonose, S.; Taguchi, T.; Mizuma, K.; Fuke, K. *Eur. J. Phys. D* **1999**, *9*, 309.
(43) Dunning, T. H., Jr. *J. Chem. Phys.* **1989**, *90*, 6117.
(44) Frisch, M. J.; Trucks, G. W.; Schlegel, H. B.; Scuseria, G. E.; Robb, M. A.; Cheeseman, J. R.; Zakrzewski, V. G.; Montgomery, J. A.; Stratmann, R. E.; Burant, J. C.; Dapprich, S.; Millam, J. M.; Daniels, A. D.; Kudin, K. N.; Strain, M. C.; Farkas, J.; Tomasi, O.; Barone, V.; Cossi, M.; Cammi, R.; Mennucci, B.; Pomelli, C.; Adamo, C.; Clifford, S.; Ochterski, J.; Petersson, G. A.; Ayala, P. Y.; Cui, Q.; Morokuma, K.; Malick, D. K.; Rabuck, A. D.; Raghavachari, K.; Foresman, J. B.; Cioslowski, J.; Ortiz, J. V.; Stefanov, B. B.; Liu, G.; Liashenko, A.; Piskorz, P.; Komaromi, I.; Gomperts, R.; Martin, R. L.; Fox, D. J.; Keith, T.; Al-Laham, M. A.; Peng, C. Y.; Nanayakkara, A.; Gonzalez, C.; Challacombe, M.; Gill, P. M. W.; Johnson, B. G.; Chen, W.; Wong, M. W.; Andres, J. L.; Head-Gordon, M.; Replogle, E. S.; Pople, J. A. *Gaussian 98*, *Revision A.5*; Gaussian, Inc.: Pittsburgh, PA, 1998.
(45) Pudzianowski, A. T. *J. Chem. Phys*. **1995**, *102*, 8029.
(46) Platts, J. A.; Laidig, K. E. *J. Phys. Chem*. **1995**, *99*, 6487.
(47) Meot-Ner (Mautner), M. *J. Am. Chem. Soc*. **1984**, *106*, 1257.
(48) Willey, K. F.; Yeh, C. S.; Robbins, D. L.; Pilgrim, J. S.; Duncan, M. A. *J. Chem. Phys*. **1992**, *97*, 8886.
(49) Scurlock, C. T.; Pullins, S. H.; Reddic, J. E.; Duncan, M. A. *J. Chem. Phys.* **1996**, *104*, 4591.
(50) Park, J. K.; Iwata, S. *J. Phys. Chem*. **1997**, *101*, 3613.
(51) Pudzianowskii, T. *J. Phys. Chem*. **1996**, *100*, 4781.
(52) Jarroszewski, L.; Lesyng, B.; Tanner, J. J.; McCammon, J. A. *Chem. Phys. Lett*. **1990**, *175*, 282.
(53) Lutz, K.; Scheiner, S. *J. Chem. Phys*. **1992**, *97*, 7507.
(54) Stanton, R. V.; Merz, K. M., Jr. *J. Chem. Phys*. **1994**, *101*, 6658.
(55) Daigoku, k.; Miura, N.; Hashimoto, K. *Chem. Phys. Lett*. In press.
(56) Payzant, J. D.; Cunnungham, A. J.; Kebarle, P. *Can. J. Chem*. **1973**, *51*, 3242.
(57) Arshadi, M. R.; Futrell, J. H. *J. Phys. Chem*. **1974**, *78*, 1482.